Ceramics International 30 (2004) 1279–1282

CERAMICS INTERNATIONAL

www.elsevier.com/locate/ceramint

Fabrication and characterization of perovskite $CaZrO_3$ oxide thin films

T. Yu [a], C.H. Chen [a], X.F. Chen [a], W. Zhu [a,*], R.G. Krishnan [b]

[a] *Microelectronics Center, School of Electrical and Electronic Engineering, Nanyang Technological University, Singapore 639798, Singapore*
[b] *Singapore Institute of Microelectronics, 11 Science Park Road, Singapore 117685, Singapore*

Received 26 November 2003; received in revised form 30 November 2003; accepted 22 December 2003

Abstract

Perovskite $CaZrO_3$ oxide thin films were prepared by the sol–gel wet chemical technology to explore the possibility of $CaZrO_3$ to be used as a gate material for MOSFET application. Calcium acetate, $Ca(CH_3COO)_2$ and zirconium acetylacetone, $[CH_3COCH{=}C(O{-})CH_3]_4Zr$ were chosen as precursors, diluted in acetic acid CH_3COOH, then mixed and stirred to get the clear and transparent solution with desired ratio of Ca:Zr = 1:1. The spin-coating technique was then used to deposit perovskite $CaZrO_3$ oxide thin films on $Pt/Ti/SiO_2/Si$ substrates, the wet films were then pyrolyzed and annealed at different temperatures under O_2 atmosphere. These thin films were systematically characterized using differential thermal analysis (DTA), thermogravimetric analysis (TGA), infrared spectra (IR), X-ray diffraction (XRD), and electrical and dielectric measurements. The high dielectric constant, low leakage current density, and high breakdown strength suggest that $CaZrO_3$ thin films can be used in high-*k* applications.

Keywords: A. Films; A. Sol–gel processes; C. Dielectric properties; D. Perovskites

1. Introduction

Aggressive scaling of gate oxide thickness for nanoscale complementary metal-oxide-semiconductor (CMOS) technology has raised more and more attention recently. The major problems associated with decreased oxide thickness are a significant increase of gate leakage current due to direct tunneling in ultrathin gate oxide. Furthermore, SiO_2 is not a good diffusion barrier for gate electrode dopants, such as boron. One efficient way to solve these problems is to go for an alternate dielectric better than SiO_2. Insulators with higher dielectric constants offer potential for increased capacitance in physically thicker films. Many materials have been investigated to replace SiO_2 as possible gate dielectrics, such as HfO_2 [1], ZrO_2 [2,3], $SrTiO_3$ [4], etc.

Metal oxides with the ABO_3 perovskite structure are of fundamental interest and significance for their electrical properties including ferroelectricity, piezoelectricity, and superconductivity and they also offer interesting high temperature properties. Alkaline-earth zirconates (such as $CaZrO_3$) are in general chemically stable and have high dielectric constant. Their perovskite structure, high-temperature properties and high dielectric constant make them promising candidates to serve as a gate material. There is little work that has been done on $CaZrO_3$ perovskite oxides for its possible application in nanoelectronic devices. In this paper, we report in detail the properties of $CaZrO_3$ thin films using the sol–gel method.

2. Experiment

$CaZrO_3$ thin films were prepared using the sol–gel wet chemical technology. Calcium acetate and zirconium butoxides were chosen as precursors, separately and thoroughly dissolved in glacial acetic acid by stirring and heating at a temperature of 60 °C, then mixed and stirred at room temperature to get a clear and transparent solution with desired mole ration of Ca:Zr = 1:1. Spin-coating technique was employed to deposit the solution onto $Pt/Ti/SiO_2/Si$ substrates. Later on, the deposited films were dried and post-annealed in an environment controllable tube furnace at temperatures ranging from 550 to 700 °C for 1 h in O_2 and air atmosphere.

---

* Corresponding author.
E-mail address: fishting@pmail.ntu.edu.sg (W. Zhu).

0272-8842/$30.00 © 2004 Elsevier Ltd and Techna Group S.r.l. All rights reserved.
doi:10.1016/j.ceramint.2003.12.037

Top electrodes of Au with a diameter of 0.3 mm were evaporated for electrical measurement.

The decomposition behavior of the dried precursor was studied using program controlled thermogravimetric analysis (TGA) and differential thermal analysis (DTA) up to a temperature of 1000 °C with a heating rate of 2 °C/min. For the DTA analysis, Al_2O_3 powder was used as a reference. The X-ray diffraction (XRD) analysis was used to study the different phases in the calcined powder at temperatures between 150 and 1000 °C and investigate the crystalline structure of the $CaZrO_3$ thin films. The Flourier transform infrared (FT-IR) reflectivity spectroscopy was used to study phase transformation mechanism. Capacitance (*C*) and leakage current density (*J*) were measured by a HP 4284A LCR meter and a HP 4155B semiconductor parameter analyzer, respectively.

3. Results and discussion

The decomposition behavior of the dried precursor was studied using thermogavimetry analysis and differential thermal analysis. Fig. 1 shows the DTA and TGA results of the $CaZrO_3$ powder. The DTA results indicate that there are two main endothermic peaks at 56 and 180 °C. The endothermic peaks and corresponding weight loss deduced from the TGA curve are attributed to the evaporation of adsorbed water and solvents. The exothermic peak at 378 °C is ascribed to the decomposition of the acetate complexes to carbonates. This decomposition causes a continuous decrease in sample weight in this temperature region. At 675 °C, an endothermic peak is found and attributed to the decomposition of the carbonates to oxides, accompanied by the loss of CO_2. As a result, the weight loss is nearly constant beyond 700 °C in the TGA curve, which indicates that the organic components and hydrates are almost completely removed. It can be seen that the crystallization temperature for the $CaZrO_3$ perovskite phase is relatively high.

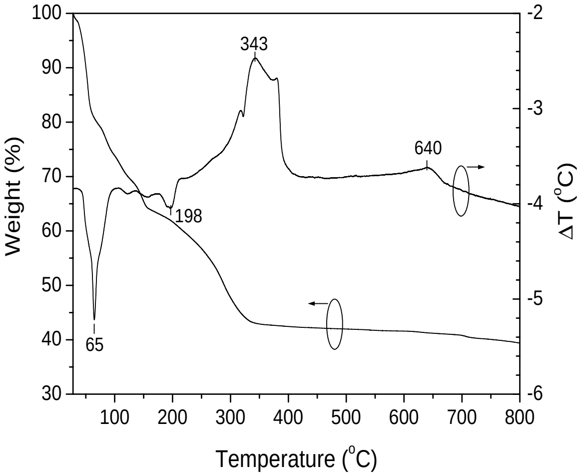

Fig. 1. DTA and TGA curves of the $CaZrO_3$ precursor at a heating rate of 2 °C/min in air.

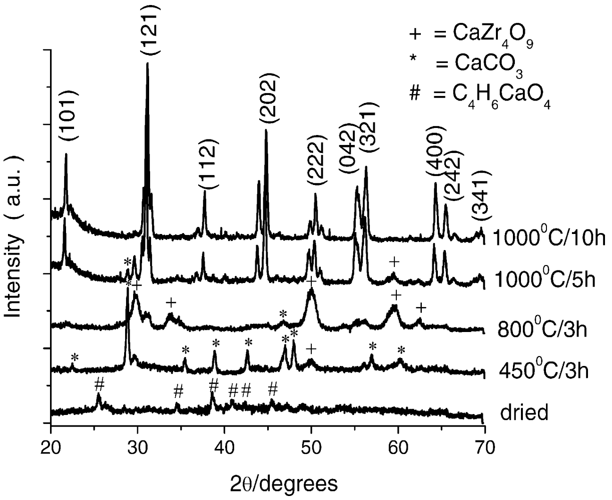

Fig. 2. XRD patterns of the $CaZrO_3$ precursor calcined at different temperatures between 150 and 1000 °C. The labeled peaks are $CaZrO_3$ phase.

Fig. 2 shows the XRD spectra taken after calcining the precursor at 150 (1 h) (drying), 450 (3 h), 800 (3 h), 1000 (5 h), 1000 °C (10 h). All peaks with # mark observed for the dried precursor can be attributed to calcium acetate ($C_4H_6CaO_4$). When the precursor is calcined at 450 °C, the calcium acetate complex decomposes to calcium carbonate, confirming the experimental results from the TG-DTA measurements. In the precursor calcined at 800 °C, two different phases are identified, a $CaZrO_3$ perovskite phase and a $CaZr_4O_9$ cubic phase. If the precipitated precursor is calcined at 1000 °C, then the solid state reactions progress even further towards formation of the desired $CaZrO_3$ phase, as shown in Fig. 2 of the XRD pattern obtained after calcining the precursor for 5 h at 1000 °C. It can be easily seen that the XRD peaks of the $CaZrO_3$ perovskite phase have increased in intensity. The intensity of the $CaZr_4O_9$ phase has decreased dramatically, indicating a substantial decrease in the amount of this phase. If the precursor is calcined at 1000 °C for 10 h, the conversion to $CaZrO_3$ phase progresses further and the $CaZr_4O_9$ phase nearly cannot be detected.

Fig. 3 shows the XRD patterns of annealed $CaZrO_3$ thin films annealed in a series of temperatures at 550, 600, 650, and 700 °C for 1 h in pure oxygen atmosphere. It is clearly shown that the film annealed at 550 °C, which is much below the crystallization temperature from the DTA analysis, has its amorphous structure. It seems that the $CaZrO_3$ film begins to crystallize at 600 °C. With further increasing the annealing temperatures, XRD results indicate that those films increase the intensity of perovskite $CaZrO_3$ phase, it means that the crystallization progresses in $CaZrO_3$ thin films further. By the way, the peaks from TiO_2 with rutile structure indicate the Ti layer below Pt bottom electrode was oxidized in the process of annealing at temperature above 650 °C.

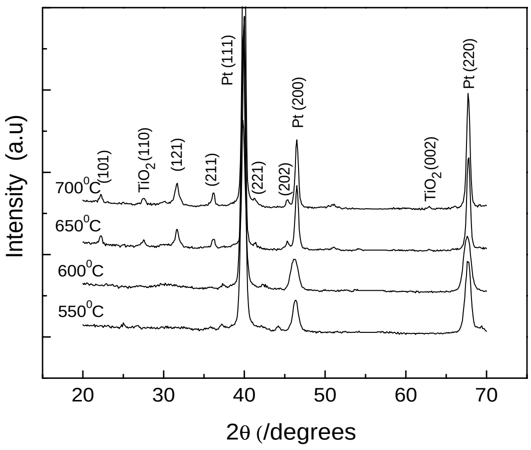

Fig. 3. XRD patterns of the $CaZrO_3$ films prepared on $Pt/Ti/SiO_2/Si$ substrates annealed at different temperatures in O_2.

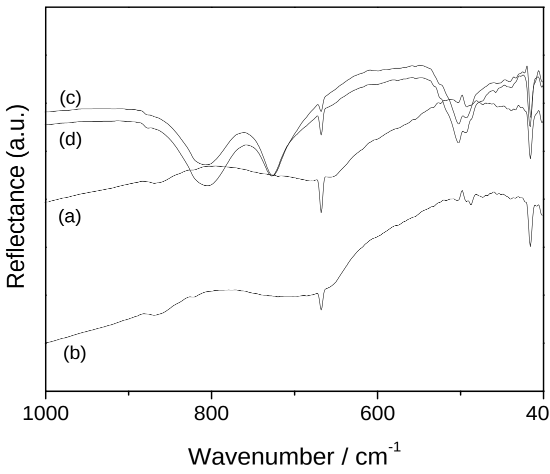

Fig. 5. FT-IR reflectivity spectra at 1000–400 cm^{-1} for $CaZrO_3$ films annealed at: (a) 550; (b) 600; (c) 650; and (d) 700 °C.

Fig. 4 shows the infrared reflectance spectra of the $CaZrO_3$ films annealed at different temperatures in the wavelength ranges of 3000–400 cm^{-1}. A bare silicon substrate was used as the reference. Three main bands are clearly shown in the spectra as follows: metal–oxygen (M–O) bonding between 400 and 800 cm^{-1}, carbon–oxygen (C–O) bonding between 1300 and 1700 cm^{-1}, and entrapped atmospheric CO_2. The 2340, 2363, and 668 cm^{-1} reflectance peaks were assigned to CO_2. When the film annealed from 550 to 700 °C, the 1409 and 1498 cm^{-1} reflectance peaks may be assigned to COO^- decreased or diminished. The C–O bonding region is indicative of organic content in the films due to the presence of residual organic carbonates at low annealing temperature. Although the carbonates are not detected by XRD, as the result, the infrared spectra (IR) indicate that the residual organic species exist in the samples heating at low annealing temperature. The further heat treatment is necessary to completely remove the organic species of residual carbonates in the films. Fig. 5 shows the detailed infrared reflectance spectra of the $CaZrO_3$ films annealed at different temperatures in the wavelength ranges of 1000–400 cm^{-1}. The reflectance peak around 805 cm^{-1} may be attributed to the longitudinal optical phonons of TiO_2, as evidenced by the emerged (0 0 2) diffraction peak due to TiO_2 in Fig. 3. The reflectance peaks at 502 and 726 cm^{-1} can be assigned as ZrO_6 octahedral stretching vibration [5] because these two peaks only exist in the samples annealing at higher temperature (650 and 700 °C). This result is agreed with the XRD results discussed in the previous section.

The characteristics of leakage current density versus applied field for capacitors of $Au/Ti/CaZrO_3/Pt$ are shown in Fig. 6. The leakage current density at room temperature fits a linear dependence of $\log J$ with $E^{1/2}$. It indicates that the Schottky emission is the dominant conduction process in the sol–gel derived $CaZrO_3$ thin films. The leakage current density of the $CaZrO_3$ thin film annealed at 650 °C for 1 h is approximately 9.5×10^{-8} A/cm^2 at high applied electrical field of 2.6 MV/cm. For the film annealed at 700 °C, the

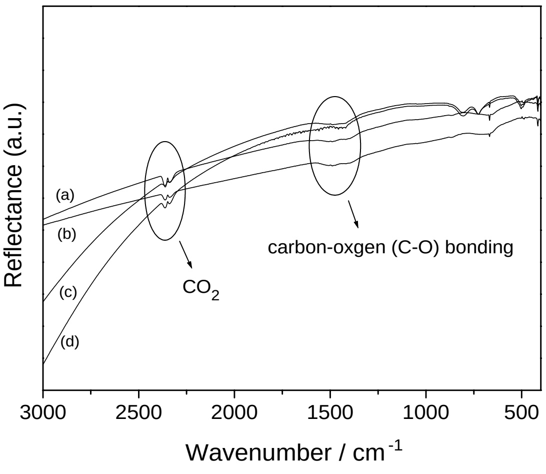

Fig. 4. FT-IR reflectivity spectra at 3000–400 cm^{-1} for $CaZrO_3$ films annealed at: (a) 550; (b) 600; (c) 650; and (d) 700 °C.

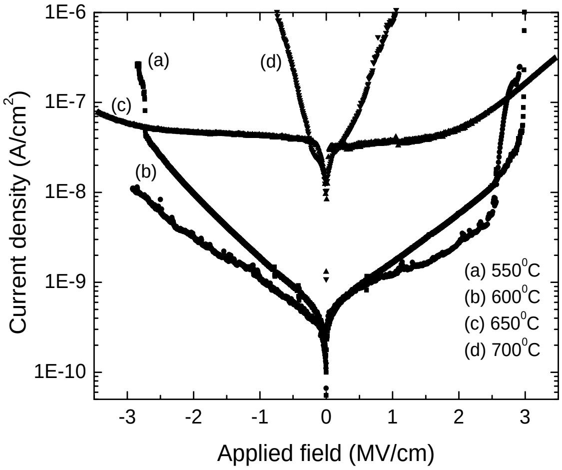

Fig. 6. Leakage current density dependence on applied field of the $CaZrO_3$ films annealed at different temperatures for 1 h in O_2.

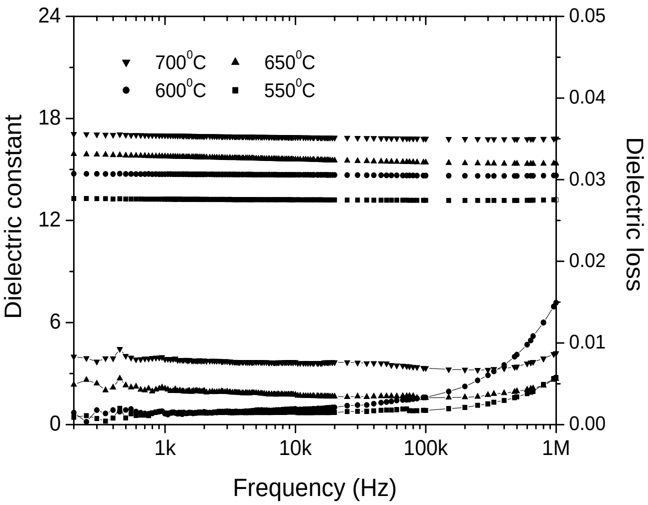

Fig. 7. Dielectric constant and dielectric loss dependence on frequency of the $CaZrO_3$ films annealed at different temperatures in O_2.

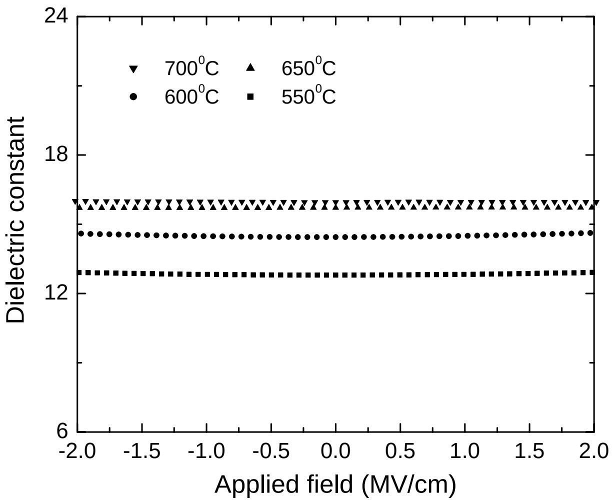

Fig. 8. Dielectric constant dependence on applied field of the $CaZrO_3$ films at a frequency of 100 kHz.

poor leakage property is attributed to some defects resulted from the polycrystalline grain growth and thus, open grain boundaries in thin films which are annealed at relatively high temperature [6].

The dielectric characteristics of $CaZrO_3$ thin films annealed at different temperatures of 550, 600, 650, and 700 °C in O_2 atmosphere as a function of frequency measured at room temperature are shown in Fig. 7. During the measurement the applied voltage was zero and the oscillation level was 50 mV. The flat curves describing the dielectric constants of these thin films exhibit very little dispersion in a frequency from 100 Hz to 1 MHz. The dielectric loss is very low for the samples annealed in O_2.

The dielectric constant dependence on the applied field is shown in Fig. 8. During the measurement the oscillation level was 50 mV and the frequency was 100 kHz. The flat curves with no significant changes in dielectric constant indicate that the dielectric constant of these samples does not depend on the applied field. Typically at a frequency of 100 kHz, the dielectric constants of those films annealed at 550, 600, 650, and 700 °C are 12.8, 14.4, 15.7, and 16.0, and the corresponding values of dielectric loss are 0.0018, 0.0027, 0.0026, and 0.0027, respectively. The dielectric constant of film annealed at 650 °C is nearly same as that of post-annealed at 700 °C. It is agreed with the XRD results that the films are crystallized more completely when the post-annealing temperature increased to 650 °C and higher. In most cases, the capacitor device requires that there is no practical change in the value of capacitance with the change in electric field. Thus, these thin films are suitable for capacitor devices of high-*k* application.

4. Summary

Perovskite $CaZrO_3$ dielectric thin films have been prepared by the sol–gel wet chemical technology, followed by post-annealing in O_2 at different temperatures from 550 to 700 °C. The phase transformation and crystallinity results show the film has amorphous structure with carbonate existing when it annealed at 550 °C. The carbonate is decomposed and those thin films crystallize into perovskite structure when annealed at 600 °C and above. The sol–gel derived $CaZrO_3$ films exhibit stable dielectric properties nearly independent from the applied electrical field and frequency at room temperature. Typically the leakage current density of the $CaZrO_3$ thin film annealed at 650 °C for 1 h is approximately 9.5×10^{-8} A/cm^2 at high applied electrical field 2.6 MV/cm. The high dielectric constant, low leakage current density and high breakdown strength suggest that the $CaZrO_3$ thin film is a promising candidate for high-k applications.

References

[1] B.H. Lee, L. Kang, R. Nieh, W.-J. Qi, J.C. Lee, Appl. Phys. Lett. 76 (2000) 1926.
[2] G.D. Wilk, R.M. Wallace, Appl. Phys. Lett. 76 (2000) 112.
[3] H. Zhang, R. Solanki, B. Roberds, G. Bai, J.C. Lee, J. Appl. Phys. 87 (2000) 1921.
[4] R. Droopad, Z. Yu, J. Ramdani, L. Hilt, J. Curless, C. Overgaard, J.L. Edwards Jr., J. Finder, K. Eisenbeiser, W. Ooms, Mater. Sci. Eng. B 87 (2001) 292.
[5] W. Zheng, W. Pang, G. Meng, Solid State Ionics 108 (1998) 37.
[6] W. Zhu, O.K. Tan, X. Yao, J. Appl. Phys. 84 (1998) 5134.